Optimal Decomposition of Stochastic Dispatch Schedule for Renewable Energy Cluster

Yue Yang, Wenchuan Wu, Bin Wang, Mingjie Li, and Tao Zhu

Abstract—The correlated renewable energy farms are usually aggregated as a cluster in economic dispatch to relieve computational burden. This strategy can also achieve better performance since the precision of predicting the power generation of a cluster can be higher than those of individual farms. This paper proposes an optimal decomposition method to allocate dispatch schedules among renewable energy farms (REFs) in the cluster under existing stochastic optimization framework. The proposed model takes advantage of probabilistic characteristics of renewable generation to minimize the curtailment and ensure the feasibility of dispatch schedule of the clusters. Approximated tractable formulation and efficient solution method are the proposed to solve the proposed model. Numerical tests show that the proposed method achieves the optimal decomposition of dispatch schedule among REFs and facilitates the utilization of renewable generation.

Index Terms—Renewable energy, stochastic optimization, economic dispatch, decomposition of dispatch schedule.

NOMENCLATURE

α	Maximal tolerable probability of total generation of renewable energy cluster (REC) exceeding upper bound of dispatch interval
β	Step length
δ	Step length to refine quantile constraint
Δ	Width of cluster dispatch interval
Ω	Subset of index set $\{1,2,...,N\}$
χ	Feasible region of problem
b_j	Binary variable
$CDF_i(\cdot)$	Cumulative density function of available generation of renewable energy farm (REF) i
$\tilde{e}_i$	Normalized forecasting error
$E(\cdot)$	Expectation of random variable
$f(\cdot)$	Total dispatch cost including fuel cost and curtailment penalty of renewable energy
$h(\cdot)$	Arbitrary convex function
K	Total number of probe points
$k_{UG,i}, k_{OG,i}$	Penalty factors of under-generation and over-generation of REF i
N	Number of renewable energy sources (RESs) in cluster
OG_i, UG_i	Over-generation and under-generation of REF i
$PDF_i(\cdot)$	Probability density function of available generation of REF i
$Q(\xi\|q)$	q-quantile of random variable ξ
$\tilde{r}$	Actual output of renewable generation
$\tilde{r}_{i,av}$	Available generation of REF i
r_i^{lb}, r_i^{ub}	Lower bound and upper bound of dispatch interval of REF i
$r_{i,forecast}$	Forecasting value of generation
$r_{i,k}$	Probe points to linearize objective function
r_i^{max}	Maximal capacity of REF i
$\boldsymbol{r}^{ub}$	Allowable upper bounds of the total renewable generation from REC
R^{lb}, R^{ub}	Lower bound and upper bound of dispatch interval of REC
$\boldsymbol{x}$	Generation schedules of conventional units

Y. Yang, W. Wu (corresponding author), and B. Wang are with the State Key Laboratory of Power Systems, Department of Electrical Engineering, Tsinghua University, Beijing 100084, China (e-mail: yangyue-thu@foxmail. com; wu-wench@tsinghua.edu.cn; wb1984@tsinghua.edu.cn).

M. Li is with the National Electric Power Control Center of State Grid Corporation of China, Beijing, China (e-mail: li-mingjie@sgcc.com.cn).

T. Zhu is with the Kunming Electric Power Supply Company of Yunnan Power Grid Corporation, Kunming, China (e-mail: taozh78@163.com).

I. INTRODUCTION

THE installed capacity of renewable energy in the power system has increased rapidly in recent years. The power output of renewable energy sources such as wind power and solar power is heavily influenced by weather conditions with significant uncertainties. Thus, novel paradigms of optimization have been introduced to model the influence of uncertainties on the operation of power system, including robust optimization (RO) and stochastic optimization (SO). Compared with conventional deterministic operation strategies, the uncertainties of renewable energy are explicitly considered in RO and SO models to arrange dispatch schedules for renewable energy sources and conventional units. The uncertainties of renewable generation are usually modelled as in-

tervals [1]-[4] or scenarios [5], [6].

Renewable energy farms (REFs) are usually integrated in power grid as aggregated renewable energy cluster (REC) based on their spatial locations, ownerships, and generation characteristics. Compared with separate operation of REF directly, the clustering of REFs is more appropriate for accommodating large-scale renewable energy because of the following advantages.

1) Clustering reduces the uncertainties and increases the predictability of renewable generation [7]. Due to the spatial smoothing effect, relative forecasting error decreases as spatial range and size of cluster expands as shown by empirical research in [8], [9]. Heterogenous clustering of REFs may further reduce the total fluctuation of power output by exploiting complementary characteristics of solar power sources and wind power sources [10].

2) Clustering provides a scalable approach for the operation and control of numerous renewable energy sources. REC participates in the dispatch at system level by replacing multiple REFs with one equivalent power source, which relieves the computational burden of economic dispatch (ED). This hierarchical dispatch framework is discussed in previous research [8], [11]-[13].

The dispatch schedules of REC should be decomposed into the instructions for each individual REF as reference for its internal generation controller. There have been some research works on the dispatch within REC. Reference [14] proposes an active power cutback control method for wind farm cluster with priority list. The regulation capacity, regulation speed, and response time are considered to choose wind farms appropriately to respond to control instructions. Two operation modes of wind farms, i. e., free mode and power restrained mode, are considered in [15], and wind farms in power restrained mode participate in active power control. Reference [11] develops a hierarchical active power dispatch framework of wind power cluster with dynamic grouping of wind farms. Reference [16] studies the active power control in photovoltaic station cluster based on the percentage of forecasting error and fairness of allocation. Reference [17] proposes an emergency controller for microgrid cluster including renewable sources.

However, there are two major technical challenges for decomposition of dispatch schedule under SO-based dispatch framework compared with conventional dispatch framework.

1) Dispatch schedule for REC under SO framework is more flexible than deterministic tracking point for generation under conventional deterministic dispatch, such as allowable generation intervals. Thus, novel decomposition model is required to allocate stochastic dispatch schedule among REFs in form of intervals.

2) Different probabilistic characteristics of REFs should be considered to obtain the appropriate decomposition strategy due to uncertainties of renewable generation. The introduction of uncertainties complicates the decomposition model and requires efficient solution method.

In order to address these issues, we propose an optimal decomposition model for stochastic dispatch schedule of REC and corresponding solution method in this paper. The major contributions of this paper are summarized as follows.

1) We develop an optimization model to enable the decomposition of more versatile dispatch schedules in form of intervals generated by stochastic dispatch framework. Uncertainties of individual REF are fully characterized with probabilistic distribution of forecasting error in the proposed models to promote the utilization of renewable energy.

2) An efficient solution method is developed for the proposed decomposition model containing nonlinear objective function and constraints by formulating a tractable optimization model with approximation. Numerical tests exhibit that our solution method scales well with the number of REFs in the cluster and is suitable for real application.

The remainder of this paper is organized as follows. The mathematical formulation of decomposition model is introduced in Section II. The solution method is developed in Section III. Numerical tests and results are demonstrated in Section IV. Conclusions are drawn in Section V.

II. MATHEMATICAL FORMULATION OF DECOMPOSITION MODEL

As shown in Fig. 1, REC plays a role as middle layer in the hierarchical operation framework of power system. From the perspective of system operator, REC participates in system-level ED and receives dispatch schedule as a whole. However, the dispatch schedules of REC cannot be executed by individual REF directly and should be allocated appropriately among REFs in the cluster, which is vital for the effective implementation of cluster-level schedules and promotes the utilization of renewable energy. Afterwards, the dispatch schedule of each REF is implemented by controlling renewable power sources such as wind turbines and photovoltaic panels. In this section, we introduce the stochastic dispatch model and decomposition model for its dispatch schedule in form of dispatch interval (DIs).
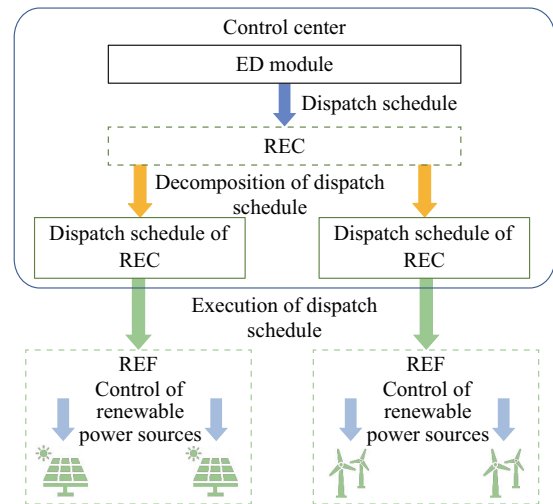

Fig. 1.   Hierarchical operation framework of power system.

A. Introduction of Stochastic ED

In this paper, we consider the stochastic ED model formulated as chance-constrained programming problem as proposed in [18], [19], which can be written in the following

compact form (1). The decision variables consist of two parts: $\boldsymbol{x}$ and $\boldsymbol{r}^{ub}$. Security constraints $g_i(\boldsymbol{x},\tilde{\boldsymbol{r}})\leq c_i$ are ensured to be satisfied with high probability when the actual output of renewable generation $\tilde{r}$ changes. $f(\boldsymbol{x},\boldsymbol{r}^{ub})$ denotes the objective function.

$$\begin{cases} \min f(\boldsymbol{x},\boldsymbol{r}^{ub}) \\ \text{s.t. } \Pr(g_i(\boldsymbol{x},\tilde{\boldsymbol{r}})\leq c_i)\geq 1-\alpha_i \\ \tilde{\boldsymbol{r}}\leq \boldsymbol{r}^{ub} \\ \boldsymbol{x},\boldsymbol{r}^{ub}\in\chi \end{cases} \tag{1}$$

B. Optimal Decomposition Model

Under the above-mentioned stochastic ED framework, the upper bound of allowable generation for REC is given as the result of optimization. Besides, the lower bound of generation from REC is inferred from aggregated cluster forecasting as the minimal generation power. Thus, the dispatch schedule of stochastic ED is provided to REC in form of DI including the allowable upper and lower bounds of generation of the entire REC. As mentioned above, the DI of individual REF needs to be determined in the decomposition procedure. Afterwards, each REF controls its generation independently according to its DI.

In order to achieve the optimal decomposition of DI, quantified criteria are required to assess the optimality of DI decomposition. Intuitively, a wider DI is better because more renewable generation in DI can be utilized. As shown in Fig. 2, renewable generation is fully accommodated without intervention when available renewable generation is between the upper and lower bounds of specified DI. If available renewable generation is less than the lower bound of DI (under-generation), spinning reserve or energy storage with fast response is required to compensate the power mismatch of the system. If available renewable generation exceeds the upper bound of DI (over-generation), necessary curtailment is introduced to keep the actual generation no higher than the allowable maximal value and ensure the system security. Thus, the upper and lower bounds of DI should be chosen to reduce the negative influence of under-generation and over-generation.
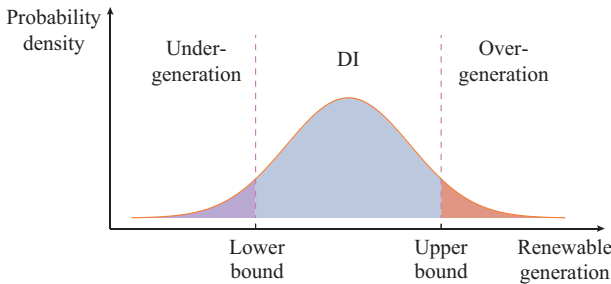

Fig. 2. Probability density function (PDF) of available renewable generation and DI.

With the notation of probability density, under-generation and over-generation under uncertainties can be represented by their expectations as:

$$E(UG_i)=\int_0^{r_i^{lb}}(r_i^{lb}-\tilde{r}_{i,av})\cdot PDF_i(\tilde{r}_{i,av})\mathrm{d}\tilde{r}_{i,av} \tag{2}$$

$$E(OG_i)=\int_{r_i^{ub}}^{r_i^{\max}}(\tilde{r}_{i,av}-r_i^{ub})\cdot PDF_i(\tilde{r}_{i,av})\mathrm{d}\tilde{r}_{i,av} \tag{3}$$

Therefore, minimizing the weighted sum of expectations of under-generation and over-generation for all REFs in the REC is selected as the objective function of the optimal DI decomposition model.

$$\min \sum_{i=1}^{N}(k_{UG,i}E(UG_i)+k_{OG,i}E(OG_i)) \tag{4}$$

We have the following constraints to ensure the feasibility of DI decomposition result. Constraints (5) and (6) ensure that the total power output of the cluster does not violate the DI constraint. Constraint (7) guarantees that the lower and upper bounds of DI are physically implementable. In practice, the sum of renewable generation is permitted to exceed the upper limit of cluster DI with a small probability α formulated as chance constraint (8), where extra generation is balanced by system-level real-time redispatch and automatic generation control procedure. The risk level α can be adjusted to promote the utilization of renewable energy, and (6) is a special case of (8) when α is 0 strictly.

$$\sum_{i=1}^{N}r_i^{lb}\geq R^{lb} \tag{5}$$

$$\sum_{i=1}^{N}r_i^{ub}\leq R^{ub} \tag{6}$$

$$0\leq r_i^{lb}\leq r_i^{ub}\leq r_i^{\max} \tag{7}$$

$$\Pr\left(\sum_{i=1}^{N}\min(\tilde{r}_{i,av},r_i^{ub})\leq R^{ub}\right)\geq 1-\alpha \tag{8}$$

The model of optimal decomposition of DI is obtained by combining objective function (4) and constraints (5), (7), and (8). The decision variables are the upper and lower bounds of DIs r_i^{ub},r_i^{lb}.

III. SOLUTION OF DECOMPOSITION MODEL

The decomposition model of DI formulated in the previous section is a nonlinear optimization problem due to the integration in objective function (2), (3), and inclusion of chance constraint (8), which is hard to solve directly. The tractable formulation and solution method of the decomposition model is discussed in this section.

A. Linearization of Objective Function

The raw probability distribution of available renewable generation can be obtained from empirical analysis on historical operation data and/or short-term numerical weather forecasting in form of probability histograms, which can be further fitted with parametric distributions such as Gaussian, Cauchy, Weibull, and beta distributions. Recently, mixture models are employed to describe the probability density of renewable generation in a more flexible and accurate approach, including Gaussian mixture model [19], versatile mixture distribution [20], and beta kernel density representation [21]. Therefore, we assume that the PDF of available re-

newable generation of each REF is known in this paper. With this assumption, the expectations in (2) and (3) can be calculated numerically for specific values of r_i^{ub}, r_i^{lb}. However, numerical integration is computationally intensive and not suitable for large-scale application.

We notice that the first-order and second-order derivatives of expected under-generation and over-generation can be expressed in cumulative probability function (CDF) and PDF of renewable generation, respectively.

$$\frac{\partial E(UG_i)}{\partial r_i^{lb}} = CDF_i(r_i^{lb}) - CDF_i(0) \tag{9}$$

$$\frac{\partial E(OG_i)}{\partial r_i^{ub}} = CDF_i(r_i^{ub}) - CDF_i(r_i^{max}) \tag{10}$$

$$\frac{\partial^2 E(UG_i)}{\partial (r_i^{lb})^2} = PDF_i(r_i^{lb}) \geq 0 \tag{11}$$

$$\frac{\partial^2 E(OG_i)}{\partial (r_i^{ub})^2} = PDF_i(r_i^{ub}) \geq 0 \tag{12}$$

The second-order derivatives are consistently nonnegative in (11) and (12), which implies that $E(UG_i)$ is a convex function of r_i^{lb} and $E(OG_i)$ is a convex function of r_i^{ub}. Inequality (13) holds for arbitrary convex function $h(x)$. Thus, the original nonlinear objective function can be approximated with series of linear constraints as shown in (15) and (16).

$$h(x) \geq h(x_0) + h'(x_0)(x - x_0) \tag{13}$$

$$\min \sum_{i=1}^{N} (k_{UG,i} s_i + k_{OG,i} t_i) \tag{14}$$

$$s_i \geq E(UG_i)\big|_{r_i^{lb} = r_{i,k}} + (CDF_i(r_{i,k}) - CDF_i(0))(r_i^{lb} - r_{i,k})$$
$$k = 1, 2, ..., K \tag{15}$$

$$t_i \geq E(OG_i)\big|_{r_i^{ub} = r_{i,k}} + (CDF_i(r_{i,k}) - CDF_i(r_i^{max}))(r_i^{ub} - r_{i,k})$$
$$k = 1, 2, ..., K \tag{16}$$

At the probe points $r_{i,k}$, the exact values of $E(UG_i)$, $E(OG_i)$ and their derivatives are evaluated in advance to formulate linear constraint as an approximation of the objective function. The appropriate selection of probe points is important for the accuracy and performance of solution. More probe points will increase the precision of linearization at the cost of more evaluations of numerical integration and more constraints in the optimization model.

Since the fluctuation of renewable generation is restricted within the range of $[0, r_i^{max}]$, the CDF at the endpoint of interval equals to 0.0 or 1.0 approximately.

$$\begin{cases} CDF_i(0) \approx 0 \\ CDF_i(r_i^{max}) \approx 1 \end{cases} \tag{17}$$

The accuracy of linear approximation is directly related to the value of second-order derivative. When the second-order derivative namely PDF of distribution is greater, the first-order approximation is less accurate and requires denser probe points. The PDF of renewable generation is usually unimodal and near zero at the edges of interval. In this paper, we propose a heuristic method to locate probe points with vari-

able probe intervals. The whole interval $[0, r_i^{max}]$ is divided into three parts at $CDF_i^{-1}(0.1)$ and $CDF_i^{-1}(0.9)$. In the leftmost and rightmost interval, probe points are selected sparsely at specific quantiles with linear or logarithmic q-values. In the central interval, denser probe points are arranged at quantiles with equidistant q-values such as 0.10, 0.12, …, 0.90. The heuristic selection of probe points achieves smaller approximation error than evenly spaced selection, which is proved by numerical test in the next section.

In practice, the linear approximation of expectations (15) and (16) can be pre-calculated by each REF in parallel. Afterwards, relevant coefficients are collected for cluster-level dispatch.

B. Approximation of Chance Constraint

The feasible region of chance constraint (8) is difficult to be expressed analytically in closed form. Although the exact feasible region can be obtained numerically via brute force search in multidimensional space, the computational complexity is exponential with respect to the number of REFs and is intractable for practical application. Instead, we give the following proposition to acquire the tractable linear constraints as its sufficient condition.

Proposition: the following inequality is a sufficient condition for chance constraint (8).

$$\sum_{i \in \Omega} r_i^{ub} + Q\left(\sum_{j \notin \Omega} \tilde{r}_{j,av} \bigg| 1 - \alpha\right) \leq R^{ub} \tag{18}$$

Proof: if $\xi_1 \leq \xi_2$ always holds for two random variables ξ_1 and ξ_2, then we have $\Pr(\xi_2 \leq c) \leq \Pr(\xi_1 \leq c)$ because $\xi_2 \leq c \Rightarrow \xi_1 \leq c$, which indicates that $\xi_2 \leq c$ is the sufficient condition of $\xi_1 \leq c$.

Inequality (20) is true due to (19). Thus, constraint (21) is a sufficient condition of (8) based on derivation above, which is equivalent to (18).

$$\begin{cases} \min(\tilde{r}_{i,av}, r_i^{ub}) \leq \tilde{r}_{i,av} \\ \min(\tilde{r}_{i,av}, r_i^{ub}) \leq r_i^{ub} \end{cases} \tag{19}$$

$$\sum_{i=1}^{N} \min(\tilde{r}_{i,av}, r_i^{ub}) \leq \sum_{i \in \Omega} r_i^{ub} + \sum_{j \notin \Omega} \tilde{r}_{j,av} \tag{20}$$

$$\Pr\left(\sum_{i \in \Omega} r_i^{ub} + \sum_{j \notin \Omega} \tilde{r}_{j,av} \leq R^{ub}\right) \geq 1 - \alpha \tag{21}$$

If $\Omega = \{1, 2, ..., N\}$ in (18), a sufficient condition is obtained, which is the same as (6). This illustrates that chance constraint (8) expands the feasible region of deterministic constraint (6).

A two-step method is developed to approach the optimal solution under chance constraint (8) approximately with help of sufficient condition proposition.

At the first step, a series of sufficient conditions are formulated by substituting Ω with different subsets in (18), and each constraint is a linear inequality with respect to r_i^{ub} after the corresponding quantile is calculated. The feasible region of original chance constraint can be approximated as a union of these linear constraints (22). It can be rewritten as mixed-integer linear constraints (23) with big-M relaxation and in-

troduction of binary variable b_j, where at least one constraint is satisfied (24).

$$\bigcup_{\Omega_j}\left\{\sum_{i\in\Omega_j}r_i^{ub}+Q\left(\sum_{j\notin\Omega_j}\tilde{r}_{j,av}|1-\alpha\right)\leq R^{ub}\right\} \tag{22}$$

$$\sum_{i\in\Omega_j}r_i^{ub}+Q\left(\sum_{j\notin\Omega_j}\tilde{r}_{j,av}|1-\alpha\right)\leq R^{ub}+(1-b_j)M \tag{23}$$

$$\sum b_j\geq 1 \quad b_j\in\{0,1\} \tag{24}$$

After solving the mixed-integer programming model including constraints (23) and (24), there must be at least one inequality constraint in (23) that is binding under optimal solution where $b_j=1$. Otherwise, $r_i^{ub}(\cdot)$ $(i\in\Omega_j)$ can further increase to reduce the objective function without violating constraint because $\dfrac{\partial E(OG_j)}{\partial r_j^{ub}}\leq 0$. Ω_j in the binding constraint represents the REFs where the generation should be restricted under the optimal decomposition of DI.

The solution obtained at the first step is conservative because the sufficient condition is stronger than original chance constraint. At the second step, we relax the binding constraint obtained from the first step gradually to refine the solution by increasing β in (25) from 0 until the chance constraint is unsatisfied. The refinement procedure contains 5 steps:

$$\sum_{i\in\Omega_j}r_i^{ub}\leq(1+\beta)\left[R^{ub}-Q\left(\sum_{j\notin\Omega_j}\tilde{r}_{j,av}|1-\alpha\right)\right] \tag{25}$$

Step 1: initialize $\beta_0=0, k=0$ and original solution x_0.
Step 2: update $\beta_{k+1}=\beta_k+\delta$.
Step 3: reoptimize original model and obtain solution x_{k+1}.
Step 4: check if the chance constraint is satisfied. If satisfied, $k=k+1$, go to *Step 2*; otherwise, go to *Step 5*.
Step 5: output the previous solution x_k as result.

Remark: the quantiles in this section can be obtained with Monte Carlo method or Gaussian mixture model (GMM) method proposed in our previous work [19].

C. Summary of Solution Procedure

Based on the approximation of nonlinear objective function and chance constraint, the overall solution procedure of optimal DI decomposition model is summarized as follows.

The model is firstly solved as mixed-integer linear programming problem including objective function (14) and constraints (5), (7), (15), (16), (23), (24), then the solution is refined iteratively by replacing (23), (24) with relaxed binding constraint (25). Especially, when the tolerable risk level α is 0, the chance constraint is equivalent to linear constraint (6) and the model is a linear programming problem.

Thus, the optimal decomposition model is transformed into tractable linear programming or mixed-integer linear programming model, and can be solved with off-shelf open-source or by commercial solvers efficiently.

IV. NUMERICAL TESTS

In this section, the proposed decomposition model of dispatch schedule and solution algorithm is tested on various cases, and the results of numerical tests are demonstrated. Firstly, a two-REF test case is discussed as a simplified example to illustrate the effectiveness of algorithm compared with the conventional decomposition method. Secondly, larger-scale test cases are constructed to exhibit the computational efficiency and scalability of the proposed solution method. Thirdly, decomposition is tested in a power system with two RECs. Optimization models are all implemented with JuMP [22] and solved by IBM CPLEX.

A. Small Test Case with Two REFs

In the first test case, we consider a cluster with two REFs. The installation capacities of REFs are both 60 MW and the forecasting values of generation are both 30 MW. $\tilde{r}_{i,av}$ is a random variable fluctuating around $r_{i,forecast}$ due to the forecasting error as shown in (26). The probability distribution of normalized forecasting error can be modelled by aggregated historical forecasting and generation data empirically. Thus, the probability distribution of available renewable generation is acquired from linear transformation of random variable.

$$\tilde{r}_{i,av}=r_{i,forecast}(1+\tilde{e}_i) \tag{26}$$

In this test case, we use normalized forecasting error distribution based on historical field data of two wind farms with one-year timespan. The probability distributions of available renewable generation from two REFs are illustrated in Fig. 3 as the probability density histograms. The mean values and standard deviations of two distributions are calculated as shown in Table I.
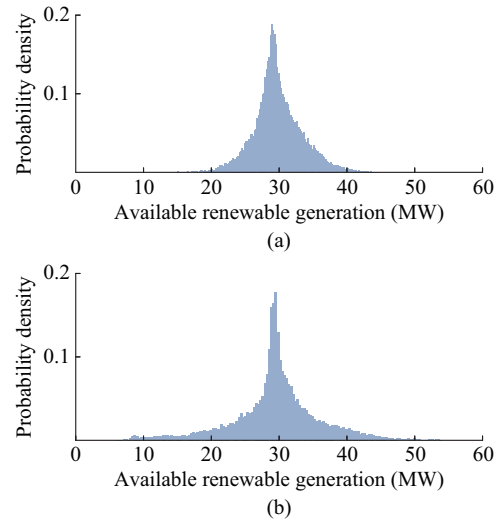

Fig. 3. Probability distributions of available renewable generation from two REFs. (a) REF 1. (b) REF 2.

The standard deviation of REF 2 is greater than that of REF 1 due to wider distribution range of forecasting errors. Thus, the expectations of under-generation and over-generation of REF 2 are higher than those of REF 1 under the same DI according to Fig. 4.

TABLE I
STATISTICS OF AVAILABLE RENEWABLE GENERATION

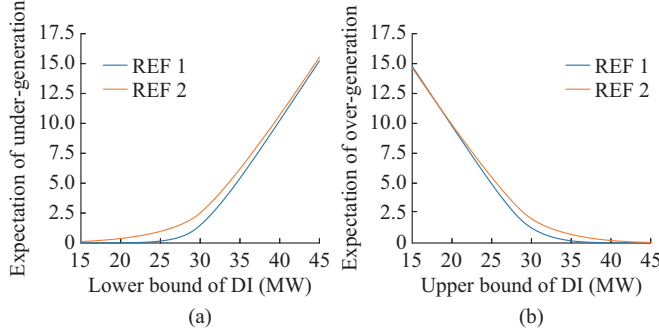| REF	Mean (MW)	Standard deviation (MW)
1	29.77	3.64
2	29.52	6.56

Fig. 4. Relationship between expectation of under-generation and over-generation and bounds of DIs. (a) Under-generation. (b) Over-generation.

Firstly, we consider the simplified version of chance constraint where the tolerable risk level is 0. The DI of cluster is provided as a result of ED and is assumed to be symmetrical with respect to the total forecasting generation 60 MW, namely $[60-\Delta/2, 60+\Delta/2]$. If no decomposition is implemented, the probability that total generation of REC stays in the DI is only 0.27, 0.49, 0.64, 0.75, 0.83 when Δ equals to 4, 8, 12, 16, 20, respectively. Therefore, the decomposition is necessary to constrain the actual generation of cluster within DI.

By setting $k_{UG,i}, k_{OG,i}$ equal to 1.0 for two REFs, the result of decomposed DIs under different values of Δ is provided in Table II, including the upper bound, lower bound, and width of DI for each REF.

TABLE II
RESULT OF DECOMPOSED DIS

Δ	REF 1 (MW)			REF 2 (MW)		
	Upper bound	Lower bound	Width	Upper bound	Lower bound	Width
4	30.75	28.95	1.80	31.25	29.05	2.20
8	31.59	28.17	3.42	32.41	27.83	4.58
12	32.30	27.63	4.67	33.70	26.37	7.33
16	33.96	26.92	6.04	35.04	25.08	9.96
20	33.75	26.60	7.16	36.25	23.40	12.84

The sum of width of individual DIs equals to Δ, which validates the correctness of the decomposition. The DI of REF 2 is consistently wider than that of REF 1, because its distribution of forecasting errors is more dispersed, and a wider DI is required to accommodate available generation and reduce the penalty of under-generation or over-generation.

Since the original nonlinear objective function is linearly approximated in our tractable optimization model, we compare the errors between approximated objective values and exact objective values (including absolute error and relative error percentage) under proposed heuristic selection of probe points with variable intervals and naive selection of probe points with uniform intervals, as shown in Table III. Both selections use 54 probe points for approximation. The proposed linear approximation achieves satisfying accuracy, and the relative error is kept under 0.2%. The selection of probe points proposed in this paper also reduces the error of approximation compared with the uniformly distributed probe points.

TABLE III
ERRORS OF OBJECTIVE VALUES COMPARED WITH EXACT OBJECTIVE VALUES

Δ	Variable intervals		Uniform intervals	
	Absolute error (MW)	Relative error (%)	Absolute error (MW)	Relative error (%)
4	−0.0010	−0.0176	−0.0413	−0.7459
8	−0.0021	−0.0489	−0.0147	−0.3462
12	−0.0016	−0.0492	−0.0216	−0.6566
16	−0.0026	−0.1031	−0.0035	−0.1394
20	−0.0036	−0.1872	−0.0106	−0.5497

If the probabilistic characteristics of forecasting errors are unknown, naive decomposition can be employed to determine DIs, which are proportional to forecasting generation of REF.

$$r_i^{ub} = \frac{r_{i,forecast}}{\sum r_{i,forecast}} R^{ub} \tag{27}$$

$$r_i^{lb} = \frac{r_{i,forecast}}{\sum r_{i,forecast}} R^{lb} \tag{28}$$

We compare the objective values of our decomposition method with naive decomposition method in Table IV. The DIs obtained from our proposed decomposition method achieve lower objective values compared with naive decomposition, because uncertainties of renewable generation from each REF are modelled explicitly in our optimal decomposition model to reduce the negative impacts of under-generation and over-generation. By contrast, DIs under naive methods are merely proportional to forecasting generation regardless of probabilistic characteristics of REFs.

TABLE IV
COMPARISON OF OBJECTIVE VALUES UNDER PROPOSED DECOMPOSITION
AND NAIVE DECOMPOSITION

Δ	Objective value (MW)	
	Proposed decomposition	Naive decomposition
4	5.5380	5.5406
8	4.2572	4.2666
12	3.2850	3.3195
16	2.5223	2.5948
20	1.9227	2.0327

$k_{UG,i}$ and $k_{OG,i}$ represent the relative priority for utilization of renewable generation among multiple REFs, and have a significant influence on the result of DI decomposition. We

test our model under two scenarios with unbalanced penalty factors where (29) and (30) holds, respectively, and the results of decomposition are shown in Tables V and VI, respectively. Compared with Table II, REF with increasing penalty factors (REF 1 in Table V, REF 2 in Table VI) receives a wider DI to promote its utilization of renewable generation. Thus, REFs with greater penalty factors are prioritized in allocation of DI. In practice, the values of penalty factors should be adjusted by system operators to obtain economically appropriate decomposition results.

$$\begin{cases} k_{UG,1} = 1.5k_{UG,2} \\ k_{OG,1} = 1.5k_{OG,2} \end{cases} \tag{29}$$

$$\begin{cases} k_{UG,2} = 1.5k_{UG,1} \\ k_{OG,2} = 1.5k_{OG,1} \end{cases} \tag{30}$$

TABLE V
RESULT OF DECOMPOSED DIs WITH $k_{UG,i}$ AND $k_{OG,i}$ SATISFYING (29)

Δ	REF 1 (MW)			REF 2 (MW)		
	Upper bound	Lower bound	Width	Upper bound	Lower bound	Width
4	31.67	28.46	3.21	30.33	29.54	0.79
8	32.32	27.60	4.71	31.68	28.40	3.29
12	33.17	26.92	6.25	32.83	27.08	5.75
16	33.75	26.21	7.54	34.25	25.79	8.46
20	34.73	25.79	8.95	35.27	24.21	11.05

TABLE VI
RESULT OF DECOMPOSED DIs WITH $k_{UG,i}$ AND $k_{OG,i}$ SATISFYING (30)

Δ	REF 1 (MW)			REF 2 (MW)		
	Upper bound	Lower bound	Width	Upper bound	Lower bound	Width
4	29.99	29.53	0.46	32.01	28.47	3.54
8	30.75	28.84	1.91	33.25	27.16	6.09
12	31.54	28.17	3.37	34.46	25.83	8.63
16	32.30	27.63	4.92	35.70	24.37	11.33
20	33.09	26.92	6.17	36.91	23.08	13.83

Next, we will consider the chance constraint with nonzero tolerable risk level. In order to calculate the probability on the left-hand side of chance constraint, we use Nataf transformation to generate scenarios of available renewable generation randomly based on marginal distribution of $\tilde{r}_{1,av}$, $\tilde{r}_{2,av}$ and their Pearson correlation coefficient, which is set to be 0.3 in this paper.

For the test case of two REFs, the feasible region of the chance constraint can be approximated by union of following three linear constraints according to mathematical derivations in Section III-B. Besides the linear approximation, the exact boundary of feasible region can also be obtained by brute force search. We plot the exact boundary and approximate boundary of feasible region at different risk levels α in Fig. 5 when R^{ub} is 70 MW. The exact feasible region is the lower left area of the solid curve and the approximate feasible region is the lower left area of the dashed curve composed of three linear segments in (31), which are both non-

convex sets. As the risk level decreases, the chance constraint becomes tighter, and the feasible region (both exact and approximate) shrinks in the lower left direction. The approximate feasible region is always a subset of the exact feasible region, which validates the sufficient condition proposition numerically.

$$\begin{cases} r_1^{ub} + Q(\tilde{r}_{2,av}|1-\alpha) \le R^{ub} \\ r_2^{ub} + Q(\tilde{r}_{1,av}|1-\alpha) \le R^{ub} \\ r_1^{ub} + r_2^{ub} \le R^{ub} \end{cases} \tag{31}$$
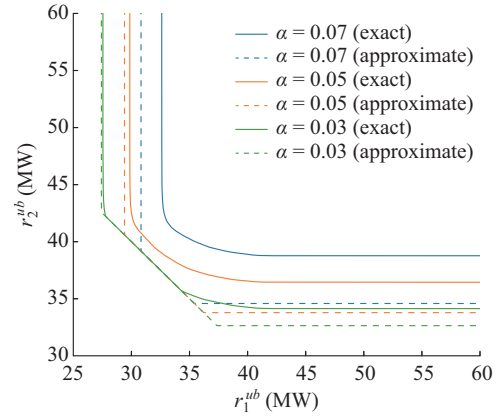

Fig. 5. Exact boundary and approximate boundary of feasible region with different confidence levels when $R^{ub} = 70$ MW.

We use $\alpha = 0.05$ as a test case with three different settings of penalty factors. The approximate solutions and refined solutions under three scenarios are shown in Fig. 6.
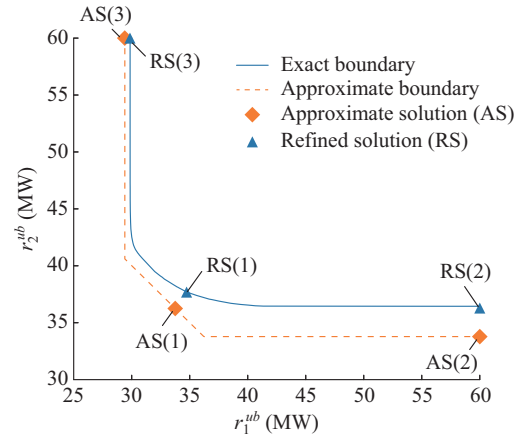

Fig. 6. Location of approximate solution and refined solution with 0.05 risk level when $R^{ub} = 70$ MW.

1) When $k_{UG,i}$ and $k_{OG,i}$ equal to 1.0 for two REFs, respectively, the optimal decomposition point in approximate feasible region is AS(1) (33.75 MW, 36.25 MW), which falls on the segment corresponding to the boundary of constraint $r_1^{ub} + r_2^{ub} \le R^{ub}$. Thus, the right-hand side of the binding constraint is increased step by step to obtain the refined solution RS(1) (34.73 MW, 37.69 MW).

2) When the penalty factor of REF 1 is 3 times that of REF 2, the optimal decomposition point in approximate feasible region is AS(2) (60.0 MW, 33.78 MW), which falls on

the segment corresponding to boundary of constraint $r_2^{ub} + Q(\tilde{r}_{1,av}|1-\alpha) \leq R^{ub}$ and indicates that only the generation of REF 2 should be restricted. The upper bound of REF 2 is lifted to 36.48 MW to reach RS(2) in the refinement procedure.

3) Similarly, when the penalty factor of REF 2 is 3 times that of REF 1, the approximated decomposition solution is AS(3) (29.4 MW, 60.0 MW), which indicates that $r_1^{ub} + Q(\tilde{r}_{2,av}|1-\alpha) \leq R^{ub}$ is the binding constraint. The upper bound of REF 1 is lifted to 29.85 MW to approach RS(3) on the exact boundary of the feasible region.

The decomposition is tested with other risk levels and their objective values are compared in Fig. 7. The objective value decreases as tolerable risk level increases because the feasible region of upper bounds of DIs is expanded to reduce curtailment and promote the utilization of renewable generation. Thus, our decomposition model is risk-adjustable to balance the security and economic cost.
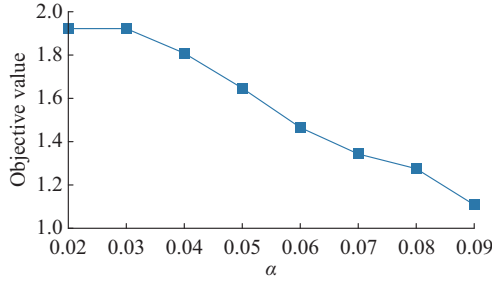

Fig. 7.   Objective values with different risk levels.

B. Test Cases with More REFs

In this subsection, test cases where the cluster contains more REFs are analyzed, and their results are discussed. We consider clusters with 10, 20, 40 and 80 REFs, and the cluster DI is [75 MW, 125 MW]. The probability distributions of available renewable generation of each REF are all based on one-year historical forecasting errors collected from real wind farms.

The computation time of optimization and comparison of objective values against naive decomposition under different numbers of REF are listed in Table VII. The computation time is under 0.05 s for cluster with 80 REFs, which illustrates the scalability of proposed decomposition model and solution method. Thus, it is suitable for real-time dispatch of large-scale RECs. The penalties of under-generation and over-generation are all reduced with our decomposed DIs compared with naive decomposition with help of explicit probabilistic modelling of uncertainties of renewable generation.

The influence of tolerable risk level is also tested, where the upper bound of cluster DI is set to be different values to simulate curtailment. We assume the tolerable risk level to be 0.01 and compare the expectation of over-generation with zero tolerable risk in Table VIII. Increasing risk level significantly reduces the curtailment of renewable generation by relaxing the constraint on the sum of DIs, and expands feasible region of decomposition. Thus, the chance-constrained formulation of decomposition model reduces the curtailment

of renewable energy as the upper bound of cluster DI can be exceeded to utilize more renewable generation.

TABLE VII
COMPARISON OF OBJECTIVE VALUES UNDER PROPOSED DECOMPOSITION AND NAIVE DECOMPOSITION

Number of REF	Computational time of proposed decomposition (s)	Objective value	
		Proposed decomposition	Naive decomposition
10	0.002	1.419	1.596
20	0.004	1.399	1.507
40	0.013	1.306	1.420
80	0.043	1.389	1.497

TABLE VIII
COMPARISON OF EXPECTATION OF OVER-GENERATION

Number of REF	With risk level of 0	With risk level of 0.01
10	2.86	0.86
20	3.87	1.26
40	4.64	1.65
80	5.46	1.98

C. Test Case with Two Clusters

In this subsection, we test the decomposition method in a 6-bus power network. There are two RECs located at different buses and each contains two REFs. The DIs of two RECs are decomposed independently. We compare the total objective values of the proposed method and naive method with different risk levels, and the results are shown in Fig. 8.
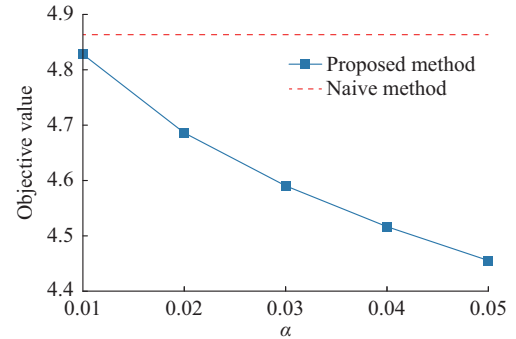

Fig. 8.   Total objective values of proposed method and naive method with different risk levels.

The optimal objective value of the proposed method consistently outperforms the result of naive method and decreases as the tolerable risk level increases, which indicates less curtailment and more utilization of renewable generation. Thus, the proposed method is applicable for multiple RECs in power systems where the decomposition of each REC is carried out in parallel.

V. CONCLUSION

A novel mathematical model for the optimal decomposition of DI of REC is proposed in this paper. The total expectation of under-generation and over-generation is minimized

as objective function based on probabilistic modelling of available renewable generation from each REF. The consistency of decomposition is ensured by the sum of lower and upper bound constraints in deterministic or chance-constrained form. We develop an efficient solution method to acquire a tractable optimization model via linear approximation of nonlinear objective function and constraints. The results of numerical test cases illustrate that the proposed decomposition model outperforms the naive decomposition due to its characterization of uncertainties of renewable generation. The computational performance and accuracy of the proposed method are also proved in the test cases.

REFERENCES

[1] C. Tang, J. Xu, Y. Sun *et al.*, "Look-ahead economic dispatch with adjustable confidence interval based on a truncated versatile distribution model for wind power," *IEEE Transactions on Power Systems*, vol. 33, no. 2, pp. 1755-1767, Mar. 2018.

[2] T. Ding, R. Bo, W. Gu *et al.*, "Absolute value constraint based method for interval optimization to SCED model," *IEEE Transactions on Power Systems*, vol. 29, no. 2, pp. 980-981, Mar. 2014.

[3] W. Wu, J. Chen, B. Zhang *et al.*, "A robust wind power optimization method for look-ahead power dispatch," *IEEE Transactions on Sustainable Energy*, vol. 5, no. 2, pp. 507-515, Apr. 2014.

[4] Z. Li, W. Wu, B. Zhang *et al.*, "Adjustable robust real-time power dispatch with large-scale wind power integration," *IEEE Transactions on Sustainable Energy*, vol. 6, no. 2, pp. 357-368, Apr. 2015.

[5] L. Wu, M. Shahidehpour, and Z. Li, "Comparison of scenario-based and interval optimization approaches to stochastic SCUC," *IEEE Transactions on Power Systems*, vol. 27, no. 2, pp. 913-921, May 2012.

[6] Y. Dvorkin, H. Pandžić, M. A. Ortega-Vazquez *et al.*, "A hybrid stochastic/interval approach to transmission-constrained unit commitment," *IEEE Transactions on Power Systems*, vol. 30, no. 2, pp. 621-631, Mar. 2015.

[7] X. Peng, Y. Chen, K. Cheng *et al.*, "Wind power prediction for wind farm clusters based on the multifeature similarity matching method," *IEEE Transactions on Industry Applications*, vol. 56, no. 5, pp. 4679-4688, Sept. 2020.

[8] Z. Lu, X. Ye, Y. Qiao *et al.*, "Initial exploration of wind farm cluster hierarchical coordinated dispatch based on virtual power generator concept," *CSEE Journal of Power and Energy Systems*, vol. 1, no. 2, pp. 62-67, Jun. 2015.

[9] M. Yang, L. Zhang, Y. Cui *et al.*, "Investigating the wind power smoothing effect using set pair analysis," *IEEE Transactions on Sustainable Energy*, vol. 11, no. 3, pp. 1161-1172, Jul. 2020.

[10] G. Yan, Z. Wang, J. Li *et al.*, "Research on output power fluctuation characteristics of the clustering photovoltaic-wind joint power generation system based on continuous output analysis," in *Proceedings of 2014 International Conference on Power System Technology*, Chengdu, China, Oct. 2014, pp. 2852-2857.

[11] L. Ye, C. Zhang, Y. Tang *et al.*, "Hierarchical model predictive control strategy based on dynamic active power dispatch for wind power cluster integration," *IEEE Transactions on Power Systems*, vol. 34, no. 6, pp. 4617-4629, Nov. 2019.

[12] S. Huang, Q. Wu, Y. Guo *et al.*, "Bi-level decentralised active power control for large-scale wind farm cluster," *IET Renewable Power Generation*, vol. 12, no. 13, pp. 1486-1492, Jul. 2018.

[13] L. Yuan, K. Meng, and Z. Y. Dong, "Hierarchical control scheme for coordinated reactive power regulation in clustered wind farms," *IET Renewable Power Generation*, vol. 12, no. 10, pp. 1119-1126, Jul. 2018.

[14] L. Lin, Y. Xie, and N. Wang, "Priority list method for active power

cutback control in a wind farm," in *Proceedings of IEEE PES Innovative Smart Grid Technologies*, Tianjin, China, May 2012, pp. 1-5.

[15] L. Lin, D. Li, C. Zhu *et al.*, "An active power control application in a utility wind farm cluster," in *Proceedings of 2014 IEEE PES General Meeting | Conference & Exposition*, National Harbor, USA, Jul. 2014, pp. 1-5.

[16] Z. Liang, Q. Linan, G. Luming *et al.*, "An active power control strategy for large-scale clusters of photovoltaic power stations," in *Proceedings of 2014 IEEE PES General Meeting | Conference & Exposition*, National Harbor, USA, Jul. 2014, pp. 1-5.

[17] M. Batool, F. Shahnia, and S. M. Islam, "Multi-level supervisory emergency control for operation of remote area microgrid clusters," *Journal of Modern Power Systems and Clean Energy*, vol. 7, no. 5, pp. 1210-1228, Sept. 2019.

[18] X. Zhu, Z. Yu, and X. Liu, "Security constrained unit commitment with extreme wind scenarios," *Journal of Modern Power Systems and Clean Energy*, vol. 8, no. 3, pp. 464-472, May 2020.

[19] Y. Yang, W. Wu, B. Wang *et al.*, "Analytical reformulation for stochastic unit commitment considering wind power uncertainty with gaussian mixture model," *IEEE Transactions on Power Systems*, vol. 35, no. 4, pp. 2769-2782, Jul. 2020.

[20] C. Tang, J. Xu, Y. Sun *et al.*, "A versatile mixture distribution and its application in economic dispatch with multiple wind farms," *IEEE Transactions on Sustainable Energy*, vol. 8, no. 4, pp. 1747-1762, Oct. 2017.

[21] B. Khorramdel, A. Zare, C. Y. Chung *et al.*, "A generic convex model for a chance-constrained look-ahead economic dispatch problem incorporating an efficient wind power distribution modeling," *IEEE Transactions on Power Systems*, vol. 35, no. 2, pp. 873-886, Mar. 2020.

[22] I. Dunning, J. Huchette, and M. Lubin, "JuMP: a modeling language for mathematical optimization," *SIAM Review*, vol. 59, no. 2, pp. 295-320, Jan. 2017.

Yue Yang received the B.S. degree from the Electrical Engineering Department, Tsinghua University, Beijing, China, in 2017. He joined the State Key Laboratory of Power Systems, Beijing, China, in September 2017, where he is currently working toward the Ph.D. degree. His research interests include optimization and control in power system with integration of renewable energy.

Wenchuan Wu received the B.S., M.S., and Ph.D. degrees from the Electrical Engineering Department, Tsinghua University, Beijing, China, in 1996, 1998, and 2003, respectively. He is currently a Professor with Tsinghua University and the Deputy Director of State Key Laboratory of Power Systems, Beijing, China. He was a Recipient of the National Science Fund of China Distinguished Young Scholar Award in 2017. His research interests include energy management system, active distribution system operation and control, machine learning and its application in energy system.

Bin Wang received the B. S. and Ph. D. degrees in electrical engineering from Tsinghua University, Beijing, China, in 2005 and 2011, respectively. He is currently a Research Scientist with the Department of Electrical Engineering, Tsinghua University. His research interests include optimal dispatch and control of renewable energy, and automatic voltage control.

Mingjie Li received the Ph.D. degree in electrical engineering from Tsinghua University, Beijing, China, in 1993. He is currently the Director of the National Electric Power Control Center of State Grid Corporation of China, Beijing, China. His research interests include operation, control and stability analysis of power systems.

Tao Zhu received the Ph.D. degree in electrical engineering, Harbin Institute of Technology, Harbin, China, in 2007. He is currently the Director-General of the Electric Power Dispatching Control Center of Kunming Power Supply Bureau, Kunming, China. His research interests include operation and control of power systems.